IIETA International Information and Engineering Technology Association
Advancing the World of Information and Engineering

Journal Européen des Systèmes Automatisés
Vol. 56, No.2, April, 2023, pp. 281-289
Journal homepage: http://iieta.org/journals/jesa

Design and Implementation of Adaptive Backstepping Control for Position Control of Propeller-Driven Pendulum System

Ahmed Khalaf Hamoudi, Luay Thamir Rasheed*

Control and Systems Engineering Department, University of Technology, Baghdad 10066, Iraq

Corresponding Author Email: luay.t.rasheed@uotechnology.edu.iq

https://doi.org/10.18280/jesa.560213

Received: 17 March 2023
Accepted: 5 April 2023

Keywords:
Backstepping Controller (BSC), Propeller-Driven Pendulum System (PDPS), Adaptive Back-stepping Controller (ABSC)

ABSTRACT

The performance of the classical and adaptive backstepping control schemes for the angular position control of a nonlinear Propeller-Driven Pendulum System (PDPS) is investigated in this paper. A Particle Swarm Optimization (PSO) algorithm has been utilized to tune the design parameters of the proposed controllers. Based on the Lyapunov stability analysis the classical and the Adaptive Back-Stepping Controllers have been constructed in order to prove the convergence of the system's error with time. The Adaptive Backstepping Controller (ABSC) is designed to compensate for the variation in the system's mass magnitude. In terms of system transient response, a comparison study of the effectiveness of both controllers has been presented in this work. The simulation results have been obtained based on the MATLAB software. In addition, a comparison study between the proposed controllers and other controllers has been listed to demonstrate the effectiveness of the proposed controller. The simulation results show that the PSO based classical Backstepping Controller (BSC) has a better performance in terms of reducing the settling time, the steady-state error, and the Root Mean Square Error ($RMSE$) value in comparison with the STSMC and SMC. In addition, the simulation results reveal that the PSO based ABSC has a better performance in terms of reducing the steady state error and the maximum overshoot in comparison with the PSO based BSC and ASTSMC.

1. INTRODUCTION

The PDPS is considered a suspended pendulum, which has a motorized propeller that generates a thrust force at the end of a pendulum rod. This thrust force has the capability of moving the pendulum up and down [1, 2]. Various control methods can be used to stabilize the pendulum at any desired position by utilizing this thrust force [3-5]. The PDPS is considered a simple plant model that is used in the education of mechatronics and mechanical engineering to explain the system dynamics and control topics. The motivation for this work is that this system has many applications such as measurement, coupled pendulum applications, special aircraft, entertainment purposes, etc. Thus, it is very important to know how to control the PDPS because this can enable us how to control its behavior, such as stability, overshoots, rise time etc. The following literature focuses on the most relevant works for PDPS control and application.

Mohammadbagheri and Yaghoobi [5] applied a PID control design to control the angular position of the PDPS. The limitation of this work is that the design parameters of the PID controller are determined using a try-and-error procedure. Kizmaz et al. [6] suggested a sliding mode control method for controlling the angular position of this system and the suggested method gives good results because this method is based on the improvement of systems robustness. The limitation of this control method is the chattering problem in the voltage control signal and the high settling time of the controlled system. Raju et al. [7] proposed a Quadratic Dynamic Matrix Control (QDMC) method to control a PDPS. This work depends on linearized the model and then deriving the transfer function of this model. The proposed method shows the ability of stabilizing the PDPS. Mohamad Reza Khoygani et al. [8] suggested the design of many controllers such as a conventional PID controller, PID-based LQR controller, Fuzzy Logic Controller (FLC), and Self-Tuning Fuzzy PID controller (STFP) for controlling the position of the PDPS.

An effective procedural control scheme is a backstepping control method, which is created in accordance with iterative phases that come to an end when the controller reaches the intended state's channel. Simulated controllers are applied to transitional state variables during the design procedure control [9]. The idea of converging in the event of uncertainty, like an effort of perturbation, is going to be distinct from the certainty scenario, necessitating previous knowledge of both the systems' characteristics and uncertainty. The primary goal of the present work is to use the optimal BSC and the optimal ABSC tightly to regulate the position angle of the PDPS to reach a desired position angle with the acceptable transient response and to calculate the disturbance. The PSO algorithm has been used in this work for tuning the gains of the proposed controllers because the try-and-error method in setting the parameters of these controllers is tedious and does not give a high-quality performance for these controllers.

The certainty parity control is one of the many current adaptive techniques based on adaptive law that work to predict unknown variables in order to reflect the real value of the unidentified parameters in the ABSC. The backstepping control technique combined with adaptive law, based on

Lyapunov stability analysis, produces performance characteristics that are essentially identical to those of a non-adaptive backstepping controller with resilience capabilities [10]. For the purpose of controlling the angular position of the PDPS, the functionality of the proposed ABSC is examined in the current study. In this paper the ABSC was used in order to force the PDPS to reach a steady-state angle with the desired transient response. The proposed method is dependent on the PDPS's time domain performance.

The rest of this paper is organized as follows. Section 2 presents the mathematical modelling of the PDPS. Section 3 suggests the design of the proposed controllers for the PDPS. In section 4, the PSO technique is explained. The simulation results of the system with the suggested controller are described in section 5. Finally, the conclusion of this paper has been given in section 6.

2. PROPELLER-DRIVEN PENDULUM SYSTEM

Figure 1 shows the simplified diagram of the PDPS. The motorized propeller is attached to the end of the suspended pendulum's arm. The position angle which is between the pendulum arm and the vertical axis is controlled by applying an input voltage to the electric DC motor. The control variable in this system is the angle which is located between the pendulum arm and the vertical axis and the control variable u is the input voltage to the electric DC motor.

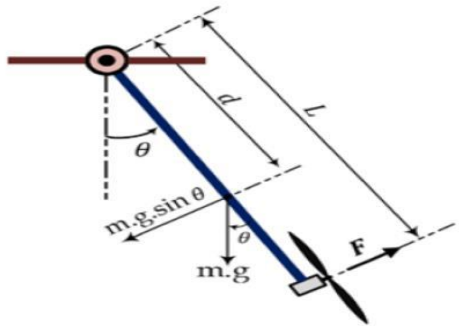

Figure 1. The PDPS's schematic diagram [3]

The nonlinear equation of motion for the PDPS is given in Eq. (1) [3, 5]:

$$J\ddot{\theta}(t) + C\dot{\theta}(t) + mdg\sin(\theta(t)) = T(t) + \varphi(t) \quad (1)$$

where, θ represents the pendulum's position angle, J represents the moment of inertia, C represents the viscous damping coefficient, d represents the length between the center of mass and the pivot point of the pendulum arm, L represents the pendulum arm length, g represents the gravitational acceleration, φ represents the external torque disturbances, m represents the pendulum mass, and T represents the thrust of the DC motor.

The rational equation between the thrust generated from the motor and the control input signal u can be expressed as in Eq. (2):

$$T(t) = K_m u(t) \quad (2)$$

where, K_m is considered as the motorized propeller constant.

By using Eq. (2), Eq. (1) can be described as follows:

$$\ddot{\theta}(t) = \frac{K_m u(t) + \varphi(t) - C\dot{\theta}(t) - mdg\sin(\theta(t))}{J} \quad (3)$$

The state $x_1(t)$ and its time derivative $x_2(t)$ are represented as below:

$$x_1(t) = \theta(t) \quad (4)$$

$$x_2(t) = \dot{x_1}(t) = \dot{\theta}(t) \quad (5)$$

Depending on Eqns. (4) and (5), Eqs. (3)-(5) are represented below:

$$\dot{x_1}(t) = x_2(t) \quad (6)$$

$$\dot{x_2}(t) = \frac{K_m u(t) + \varphi(t) - Cx_2(t) - mdg\,sin(x_1(t))}{J} \quad (7)$$

3. BACKSTEPPING CONTROLLERS DESIGN

The control law of the classical BSC is improved in this section based on adaptive backstepping methodology. Firstly, the design of the classical BSC must be carried out and then the ABSC will be established accordingly. The BSC is accountable for stabilizing and regulating the angular positions of the PDPS relative to their respective normal positions. The BSC is accountable for regulating and stabilizing the angular position of the PDPS to the desired angular position. The design procedures of both controllers are explained as follows [11-14]:

3.1 Backstepping controller

Let e_1 be the difference between the actual state x_1 and the reference position x_d:

$$e_1(t) = x_1(t) - x_d(t) \quad (8)$$

Eq. (9) can be obtained by using the time derivative of e as follows:

$$\dot{e_1}(t) = x_2(t) - \dot{x_d}(t) \quad (9)$$

The difference between the virtual controller (α) and (x_2) can be described as follows:

$$e_2(t) = x_2(t) - \alpha(t) \quad (10)$$

By substituting Eq. (10) in Eq. (9), the time derivative of e_1 can be represented as follows:

$$\dot{e_1}(t) = \alpha(t) + e_2(t) - \dot{x_d}(t) \quad (11)$$

According to Eq. (11), the virtual controller (α) is chosen as follows:

$$\alpha\,(t) = -a_1 e_1(t) + \dot{x_d}(t) \quad (12)$$

$$\alpha\,(t) = -a_1(x_1(t) - x_d(t)) + \dot{x_d}(t) \quad (13)$$

where, a_1 is a constant greater than zero.

By substituting Eq. (12) in Eq. (11), Eq. (11) becomes as follows:

$$\dot{e_1}(t) = -a_1\, e_1(t) + e_2\,(t) \tag{14}$$

Taking the time derivative of Eq. (10), gives:

$$\dot{e_2}(t) = \dot{x_2}(t) - \dot{\alpha}(t) \tag{15}$$

$$\dot{e_2}(t) = \frac{K_m}{J}u(t) - \frac{C}{J}x_2(t) - \frac{mdg}{J}sin\big(x_1(t)\big) + \frac{\varphi(t)}{J} - \dot{\alpha}(t) \tag{16}$$

The control signal can be defined as follows:

$$u(t) = \frac{J}{K_m}\,((\frac{c}{J})x_2(t) + \frac{mdg}{J}\,sin(x_1(t))\, - \frac{\varphi(t)}{J} + \dot{\alpha}(t) + \dot{e_2}(t)) \tag{17}$$

Consider the following expression for the time derivative of $(e_2(t))$ as follows:

$$\dot{e_2}(t) = -a_2 e_2(t) - e_1(t) \tag{18}$$

where, a_2 is a constant greater than zero.

The time derivative of (α) is described as follows:

$$\dot{\alpha}(t) = -a_1\dot{e_1}(t) + \ddot{x_d} \tag{19}$$

By substituting Eqs. (19), (18), (9), (8), (10), and (13) in Eq. (16), the control signal can be described as follows:

$$\begin{aligned} u(t) = \frac{\mathrm{J}}{K_m}((-a_1a_2 - 1)x_1(t) \\ - \Big(a_2 - \frac{C}{J} + a_1\Big)x_2(t) \\ + (a_1a_2 + 1)x_d(t) \\ + \frac{mdg}{J}sin(x_1(t)) - \frac{\varphi(t)}{J} \\ + (a_1 + a_2)\dot{x}_d(t) + \ddot{x}_d(t) \end{aligned} \tag{20}$$

The schematic diagram of the optimal BSC for the output angular position control of the PDPS is illustrated in Figure 2.

3.2 Adaptive backstepping controller

Suppose the uncertainty m is bounded and unknown, then by using the principle of certainty equivalence, an estimated $\hat{m}$ is substituted for the actual value of uncertainty m. The difference between these two values represents the estimation error as follows:

$$\tilde{m} = m - \hat{m} \tag{21}$$

The control signal using the uncertainty estimate value instead of the actual value of m is described as follows:

$$u(t) = \frac{J}{K_m}\,((\frac{c}{J})x_2(t) + \frac{\hat{m}dg}{J}\,sin(x_1(t))\, - \frac{\varphi(t)}{J} + \dot{\alpha}(t) + \dot{e_2}(t)) \tag{22}$$

The Eq. (23) is described as follows:

$$\dot{e_2}(t) = -c_2 e_2(t) - e_1(t) + \frac{\tilde{m}}{J} \tag{23}$$

The following Lyapunov function is chosen to develop the adaptive law:

$$V(e_1, e_2, \tilde{m}) = \frac{1}{2}e_1(t)^2 + \frac{1}{2}e_2(t)^2 + \frac{\tilde{m}^2}{2\beta} \tag{24}$$

where, β is a design parameter.

The time derivative of the chosen Lyapunov function is given as follows:

$$\dot{V}(e_1, e_2, \tilde{m}) = -e_1(t)^2 - e_2(t)^2 + \tilde{m}(\frac{e_2(t)}{J} - \frac{\dot{\hat{m}}}{\beta}) \tag{25}$$

To ensure that the preceding equation is negative-definite, the following adaptive law is derived.

$$\dot{\hat{m}} = \frac{\beta e_2(t)}{J} \tag{26}$$

The schematic diagram of the optimal ABSC for the output angular position control of the PDPS is depicted in Figure 3.

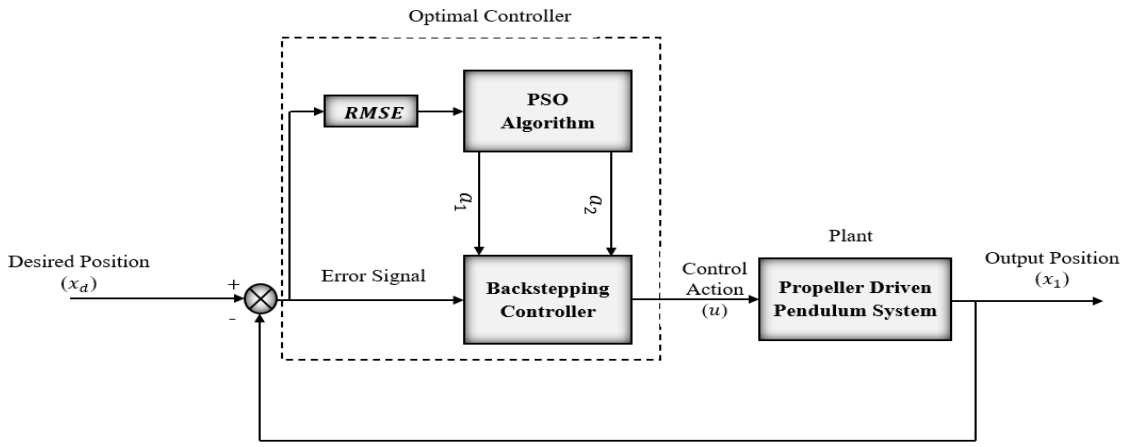

Figure 2. The scheme of the optimal BSC for controlling the output angular position of the PDPS.

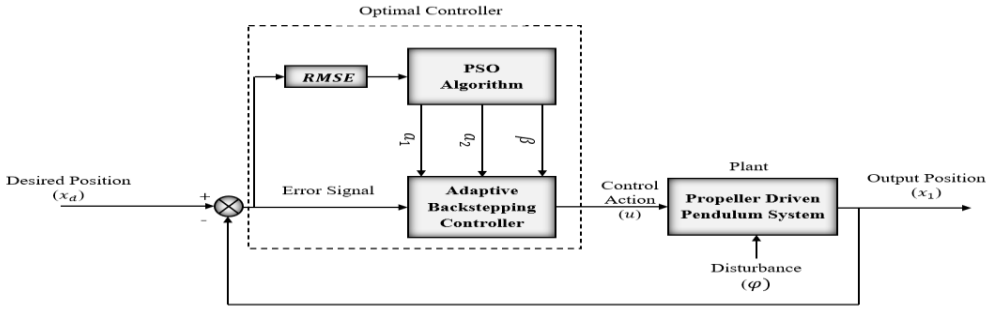

Figure 3. The scheme of the optimal ABSC for controlling the output angular position of the PDPS.

4. PARTICLE SWARM OPTIMIZATION

The PSO is an evolutionary optimization technique that was first introduced in 1995. In this technique, a particle represents a potential solution to the problem. Each particle's (bird) flight is adjusted based on its own flying experience and the flying experience of its companion. The following equations represent the updating of each bird's velocity and position [15, 16]:

$$V_i^{k+1} = wV_i^k + c_1 r_{n1}\left(p_{best_i}^k - X_i^k\right) + c_2 r_{n2}\left(g_{best}^k - X_i^k\right) \quad (27)$$

$$X_i^{k+1} = X_i^k + V_i^{k+1} \quad (28)$$

where, $i = 1, 2, \dots, N_p$, N_p is the population size, $k = 1, 2, \dots, k_{max}$, k_{max} is the maximum number of iterations, V_i^k is the velocity of the i^{th} bird, w is the inertial weight coefficient, c_1 and c_2 are the learning factors, r_{n1} and r_{n2} are random numbers between [0,1], X_i^k is the location of the i^{th} bird.

As a cost function, $RMSE$ is selected and is defined as follows [17]:

$$RMSE = \sqrt{\frac{1}{n}\sum_{i=1}^{n}(x_1 - x_d)^2} \quad (29)$$

where, x_1 is the actual position, x_d is the desired position, and n is the number of acquired samples.

The pseudocode of the PSO technique for tuning the design parameters of the proposed controllers is described below:

Pseudocode of PSO algorithm

Step 1: Set Parameters.
(a) Set the PSO parameters, including the value of the inertia factor (w), population size (N_p), learning factors (c_1 and c_2), dimension of the problem (dim), and the maximum iterations limit (k_{max}).
(b) **for** each bird $i = 1, ..., N_p$, **do**
Initialize the birds' velocity and position randomly: $V_i(0)$ and $X_i(0)$.
(c) Calculate the $RMSE$ cost function for all birds using Eq. (29).
(d) For all birds, evaluate p_{best} to their initial position: $p_{best_i} = X_i(0)$.
(e) Put the g_{best} value to the position of the bird with the lowest $RMSE$ value among all birds.
end for
Step 2: Repeat the process until the maximum iterations limit is attained.
While ($k < k_{max}$) **do**
for each bird $i = 1, 2, \dots, N_p$, **do**
Update the velocity of each bird using Eq. (27).
Update the position of each bird using Eq. (28).
Calculate the $RMSE_i$ cost function using Eq. (29).
if $\mathrm{RMSE}\left(\mathrm{X_i^{k+1}}\right) < \mathrm{RMSE}\left(\mathrm{X_i^k}\right)$.
$\mathrm{p_{best_i}} = \mathrm{X_i^{k+1}}$.
end if
if $\min(\mathrm{RMSE}(\mathrm{X^{k+1}}) < \min(\mathrm{RMSE}(\mathrm{X^k})$
$\mathrm{g_{best}} = \mathrm{X^{k+1}_{min\ (RMSE)}}$
end if
end for
$\mathrm{k = k + 1}$
end while
Step 3: Output the best solution found (g_{best}).

5. SIMULATION RESULTS

The simulation results are conducted using MATLAB software to show the effectiveness of the optimal controllers in controlling the angular position of the PDPS. The performances of the optimal proposed backstepping controllers are compared with that of the other controllers in this study. The initial values of the variables x_1 , x_2, and φ are equal to 0, 0, and 0.1 respectively. The nominal parameters of the PDPS are illustrated in Table 1 [3].

The try-and-error method in setting the parameters of the proposed controllers is tedious and does not give a high-quality performance of the proposed controllers. Therefore, in this study, a PSO technique is used to find the optimal parameters of these controllers. The parameters of the PSO algorithm are described in Table 2.

Table 1. The nominal parameters of the PDPS [3]

Parameter and Symbol	Value and Unit
Pendulum Mass (m)	0.36 kg
Motor constant (K_m)	0.0296
Length between the suspending point and the center of mass (d)	0.03 m
Acceleration due to gravity (g)	9.81 m/s^2
Moment of inertia (J)	0.0106 $kg.m^2$
Viscous damping coefficient (C)	0.0076 Nms/rad
DC motor input voltage (u)	$\pm 24\ V$

Table 2. The PSO algorithm parameters

Parameter	Value
Population size (N_p)	25
Maximum number of iterations (k_{max})	100
The cognitive learning factor (c_1)	1.49618
The social learning factor (c_2)	1.49618
the inertial weight coefficient (w)	0.7298
Dimension of the problem	2

Table 3 shows the gains of the proposed optimal controllers by using the PSO technique for the PDPS controlled. Figure 4 reveals the cost function plots with respect to iteration for the angular position of the PDPS. This figure shows that the PSO technique could reduce effectively the cost function in relation to iteration to achieve the controlled system's optimal performance.

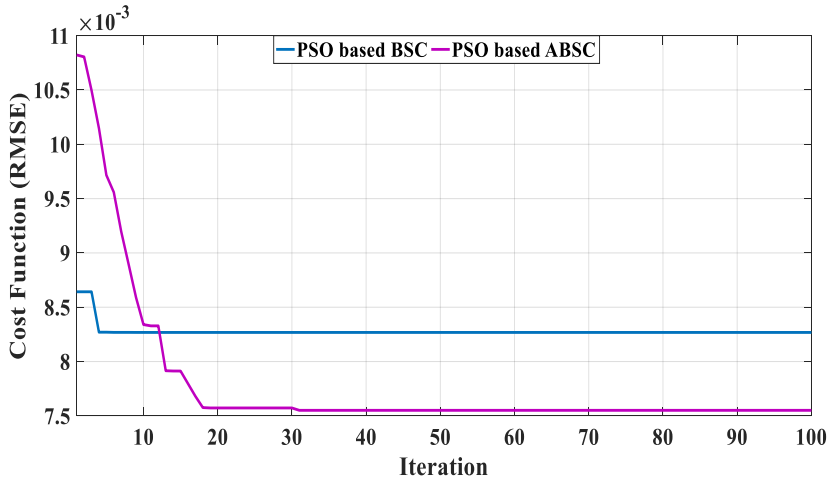

Figure 4. The cost function plots for the proposed optimal controllers

Table 3. The gains of the proposed optimal controllers using the PSO technique

Controller	Parameter	Value
PSO based BSC	a_1	25.359
	a_2	45.025
PSO based ABSC	a_1	14.652
	a_2	44.7
	β	−0.155

Scenario I: Control without mass uncertainty and external disturbance

In this part, the ABSC has been discarded because of the absence of mass uncertainty and external disturbance problems. The angular output position and velocity of the PDPS controlled by the optimal BSC are shown in Figures 5 and 6, respectively. It is clear that the dynamic response of this controlled system is better than that of (which was used in the study [3]) the other controller, especially in terms of reducing the settling time, steady state error and cost function ($RMSE$) value as shown in Table 4. The corresponding control effort due to the optimal BSC is illustrated in Figure 7. This control effort is smooth and did not exceed the saturation voltage of the DC motor.

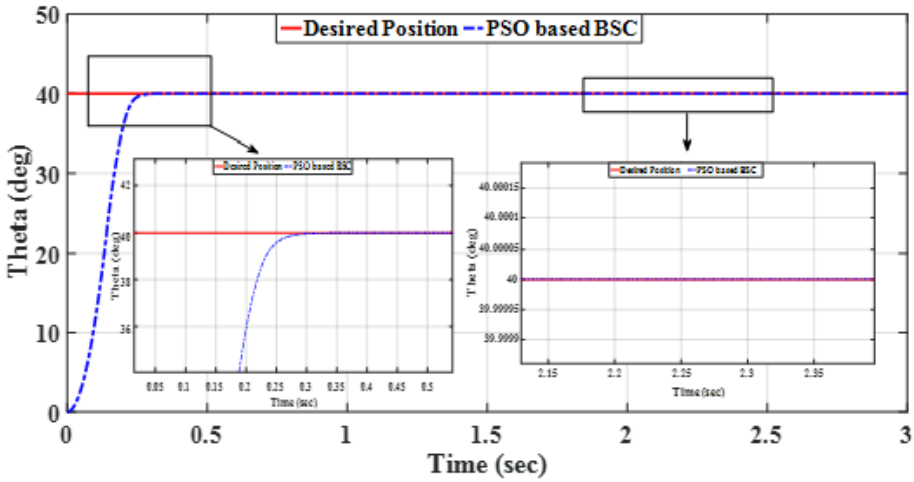

Figure 5. The dynamic behaviour of the PDPS using PSO based BSC

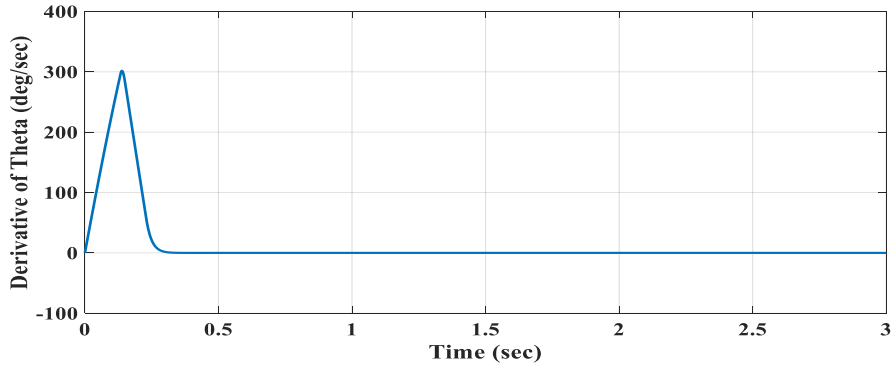

Figure 6. The angular velocity of the PDPS using PSO based BSC

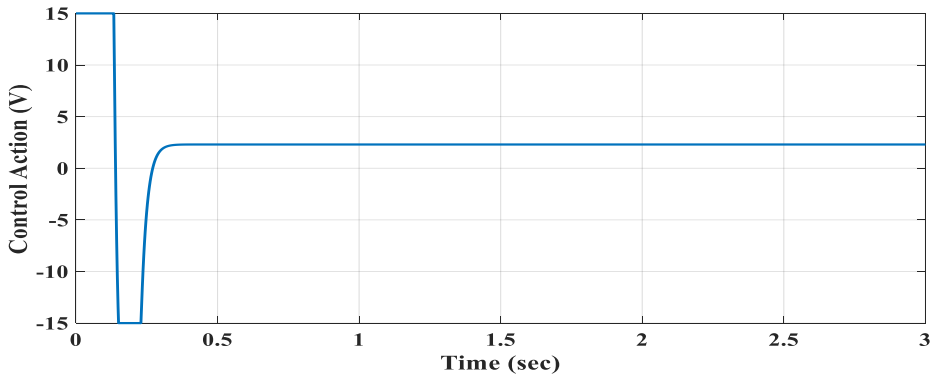

Figure 7. The voltage control signal of the controlled system based PSO based BSC

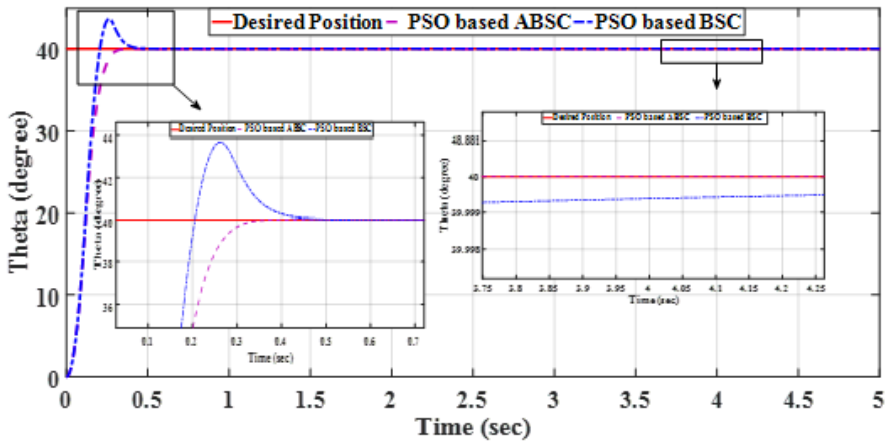

Figure 8. The dynamic behaviours of the PDPS using the proposed optimal controllers under the mass uncertainty and external disturbance

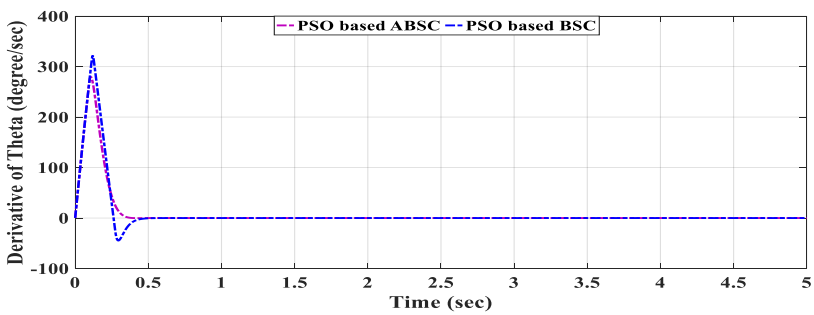

Figure 9. The angular velocities of the PDPS using the proposed optimal controllers under the mass uncertainty and external disturbance

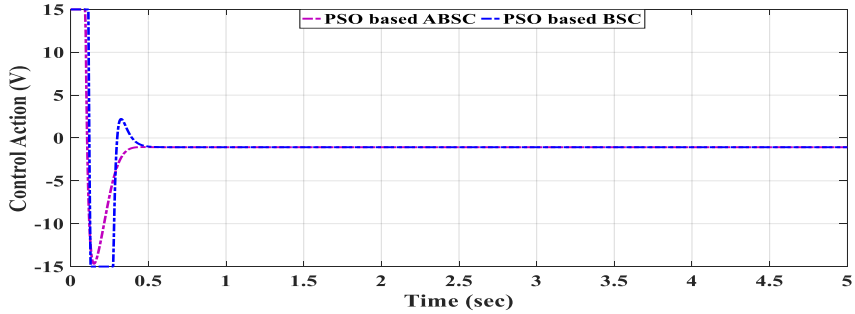

Figure 10. The voltage control signals of the controlled system using the proposed optimal controllers under the mass uncertainty and external disturbance

Table 4. The nominal controlled system dynamic performance using the proposed controllers

Controller	Settling time (sec)	Steady state error (degree)	RMSE
PSO based BSC	0.35	0	0.00827
STSMC [3]	1.26	0.1	0.1206
SMC [3]	0.88	0.13	0.08097

Scenario II: Control with mass uncertainty and external disturbance

In this part, the PSO based BSC and PSO based ABSC have been assessed under the presence of mass uncertainty and external disturbance problems. The angular output position and velocity of the PDPS controlled by the PSO based BSC and PSO based ABSC are depicted in Figures 8 and 9. Figure 8 illustrates that both optimal controllers are capable of tracking the desired trajectory while the PSO based ABSC has a better dynamic performance compared to other controllers as shown in Table 5.

Table 5. The dynamic performance of the uncertain controlled system using the proposed controllers

Controller	Settling time (sec)	Steady state error (degree)	Maximum overshoot	RMSE
PSO based ABSC	0.35	0	0	0.00761
PSO based BSC	0.205	0.0005	9.5%	0.00827
ASTSMC [3]	0.44	0.13	0	0.0682

The control signals behaviour using the proposed optimal controllers are described in Figure 10. It is evident that the responses of the control signals are smooth and within the acceptable voltage range of the pendulum system's DC motor. The estimation behaviour of the pendulum mass and the external torque disturbance are shown in Figures 11 and 12, respectively. It is evident that the estimation error of the pendulum mass may reach zero as time tends to 2.5 sec.

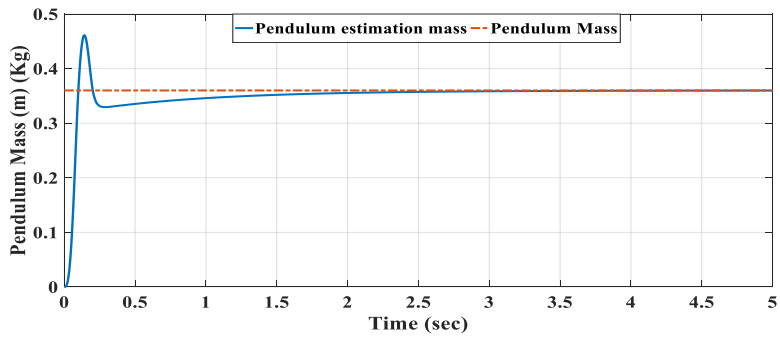

Figure 11. Pendulum estimation mass (Kg)

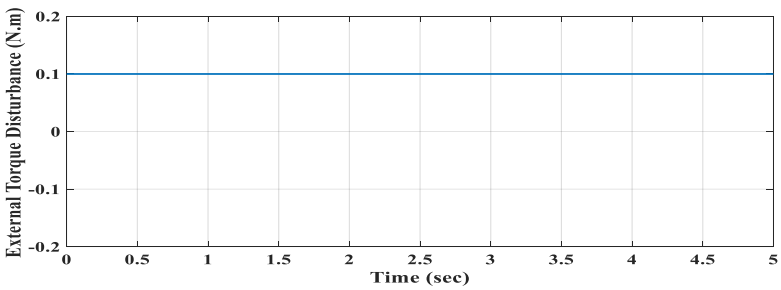

Figure 12. External torque disturbance ($N.m$)

6. CONCLUSIONS

This work presents the design of the optimal BSC and optimal ABSC for controlling the angular position of the PDPS. A controlled system's stability analysis has been presented using the Lyapunov function. The simulation results demonstrated that the PSO technique could significantly improve the proposed controllers' dynamic performance. A comparison study has been conducted between the proposed optimal controllers and other controllers. The simulation results reveal that the PSO based BSC has a better dynamic performance in comparison with the other controllers' performance such as SMC and STSMC in reducing the settling time, steady state error and $RMSE$ value [3]. In addition, the PSO based ABSC has been designed to estimate bounded mass uncertainty and to compensate for the effect of the external torque disturbance. The transient characteristics of the PSO based ABSC are better than those using PSO based BSC and ASTSMC in reducing the settling time, steady state error, maximum overshoot and $RMSE$ value.

For future work, this study can be extended by including different optimization algorithms for the purpose of comparison with the PSO technique [18-21]. In addition, another extension of this study could be by using other embedded hardware designs such as Raspberry Pi or FPGA or by using LabVIEW programming software in order to implement the proposed controller in a real-time environment [22-25].

REFERENCES

[1] Taskin, Y. (2017). Fuzzy PID controller for propeller pendulum. Istanbul University - Journal of Electrical and Electronics Engineering (IU-JEEE), 17 (1): 3175-3180.

[2] Job, M.M., Jose, P.S.H. (2015). Modeling and control of mechatronic aero pendulum. In 2015 International Conference on Innovations in Information, Embedded and Communication Systems (ICIIECS), pp. 1-5. IEEE.

[3] Al-Qassar, A.A., Al-Dujaili, A.Q., Hasan, A.F., Humaidi, A.J., Ibraheem, I.K., Azar, A.T. (2021). Stabilization of single-axis propeller- powered system for aircraft applications based on optimal adaptive control design. Journal of Engineering Science and Technology (JESTEC), 16(3): 1851-1869.

[4] Ghasemi, R., Khoygani, M.R.R. (2014). Designing intelligent adaptive controller for nonlinear pendulum dynamical system. International Journal of Computer, Information, Systems, and Control Engineering, 8(11): 1755- 1759.

[5] Mohammadbagheri, A., Yaghoobi, M. (2011). A new approach to control a driven pendulum with PID method. 13th International Conference on Modelling and Simulation, pp. 207-211. http://dx.doi.org/10.1109/UKSIM.2011.47

[6] Kizmaz, H., Aksoy, S., Mühürcü, A. (2010). Sliding mode control of suspended pendulum. Modern Electric Power Systems, pp. 1-6. IEEE.

[7] Raju, S.S., Darshan, T.S., Nagendra, B. (2012). Design of quadratic dynamic matrix control for driven pendulum system. International Journal of Electronics and Communication Engineering, 5(3): 363-370.

[8] Khoygani, M.R.R., Ghasemi R., Sanaei, D. (2013). Design controller for a class of nonlinear pendulum dynamical system. International Journal of Artificial Intelligence (IJ-AI), 2(4): 159- 168.

[9] Khalil, H.K. (2002). Nonlinear Systems. Prentice Hall: Upper Saddle River, NJ, USA.

[10] Krstic, M., Kokotovic, P.V., Kanellakopoulos, I. (1995). Nonlinear and Adaptive Control Design. Wiley: New York, NY, USA.

[11] Humaidi, A., Hameed, M. (2019). Development of a new adaptive backstepping control design for a non-strict and under-actuated system based on a PSO tuner. MDPI, Information, 10(2): 38, pp. 1-17. https://doi.org/10.3390/info10020038

[12] Al-Araji, A.S. (2015). Cognitive non-linear controller design for magnetic levitation system. SAGE Journals, Transactions of the Institute of Measurement and Control, 38(2): 1-8. https://doi.org/10.1177/0142331215581639

[13] Rasheed, L.T., Hamzah, M.K. (2021). Design of an optimal backstepping controller for nonlinear system under disturbance. Engineering and Technology Journal, 39(3): 465-476. https://doi.org/10.30684/etj.v39i3A.1801

[14] Al-Dujaili, A.Q., Humaidi, A.J., Allawi, Z.T., Sadiq, M. E. (2023). Earthquake hazard mitigation for uncertain building systems based on adaptive synergetic control. Applied System Innovation, 6(2): 1-15. https://doi.org/10.3390/asi6020034

[15] Rasheed, L.T., Yousif, N.Q., Al-Wais, S. (2023). Performance of the optimal nonlinear pid controller for position control of antenna azimuth position system. Mathematical Modelling of Engineering Problems, 10(1): 366-375. http://dx.doi.org/10.18280/mmep.100143

[16] Rasheed, L.T. (2020). Optimal tuning of linear quadratic regulator controller using ant colony optimization algorithm for position control of a permanent magnet DC motor. Iraqi Journal of Computers, Communications, Control and Systems (IJCCCE), 20(3): 29-41.

[17] Humaidi, A.J., Kadhim, S.K., Gataa, A.S. (2022). Optimal adaptive magnetic suspension control of rotary impeller for artificial heart pump. Cybernetics and Systems, 53(1): 141-167. http://dx.doi.org/10.1080/01969722.2021.2008686

[18] Waheed, Z.A., Humaidi, A.J. (2022). Design of optimal sliding mode control of elbow wearable exoskeleton system based on whale optimization algorithm. Journal Européen des Systèmes Automatisés, 55(4): 459-466. https://doi.org/10.18280/jesa.550404

[19] Rasheed, L.T. (2023). An optimal modified elman - PID neural controller design for DC/DC boost converter model. Journal of Engineering Science and Technology (JESTEC), 18(2): pp. 880-901.

[20] Hamzah, M.K., Rasheed, L.T. (2022). Design of optimal sliding mode controllers for electrical servo drive system under disturbance. AIP Conference Proceedings 2415, 030005. https://doi.org/10.1063/5.0092311

[21] Arshaghi, A., Ashourian, M., Ghabeli, L. (2020). Detection of skin cancer image by feature selection methods using new buzzard optimization (BUZO) algorithm. Journal Européen des Systèmes Automatisés,

37(2): 181-194. https://doi.org/10.18280/ts.370204
[22] Al-Dujaili, A.Q., Falah, A., Humaidi, A.J., Pereira, D.A., Ibraheem, K.I. (2020). Optimal super-twisting sliding modecontrol design of robot manipulator: Design and comparison study. SAGE Journals, International Journal of Advanced Robotic Systems, 17(6): 1-17. https://doi.org/10.1177/1729881420981524
[23] Abed, H.Y., Humaidi, A.J., Humod, A.T., Al-Dujaili, A.Q. (2019). Experimental design and implementation of IT2FL-controlled BLDCM Based on LabVIEW™. International Journal of Recent Technology and Engineering (IJRTE), 8(4): 587-592. http://dx.doi.org/10.35940/ijrte.D7319.118419
[24] Wang, J., Li, M., Jiang, W., Huang, Y., Lin, R. (2022). A design of FPGA-based neural network PID controller for motion control system. Sensors, 22(3): 889. https://doi.org/10.3390/s22030889
[25] Abdul Karim, M.Z.B, Thamrin, N.M. (2021). Servo motor controller using PID and graphical user interface on Raspberry Pi for robotic arm. IOP Publishing, International Conference on Robotic Automation System (ICORAS). http://dx.doi.org/10.1088/1742-6596/2319/1/012015

NOMENCLATURE

a_1	dimensionless constant greater than zero
a_2	dimensionless constant greater than zero
C	viscous damping coefficient, N.m.s. rad^{-1}
c_1	dimensionless cognitive learning factor
c_2	dimensionless social learning factor
d	the length between the center of mass and the pivot point of the pendulum arm, m
e_1	difference between the actual state x_1 and the reference position x_d, rad
e_2	difference between the virtual controller (α) and (x_2), rad. s^{-1}
g	gravitational acceleration, m. s^{-2}
J	moment of inertia, kg.m^2
K_m	dimensionless motorized propeller constant
L	pendulum arm length, m
m	actual pendulum mass, kg
$\widehat{m}$	an estimated mass, kg
$\widetilde{m}$	difference between the actual and estimated pendulum mass, kg
n	dimensionless the number of acquired samples
T	the thrust generated from the motor, N
u	Voltage control action, V
V	particles velocities, m. s^{-1}
w	dimensionless inertial weight coefficient
X	particles positions, m
x_d	desired position, rad
x_1	actual position, rad
x_2	actual velocity, rad. s^{-1}

Greek symbols

α	virtual controller, rad. s^{-1}
β	dimensionless design parameter
φ	external torque disturbances, N. m
θ	pendulum's position angle, rad